Eclética Química
ISSN: 0100-4670
ISSN: 1678-4618
ecletica@journal.iq.unesp.br
Universidade Estadual Paulista Júlio de Mesquita Filho
Brasil

Luiz, Jose Marques; Nunes, Ronaldo Spezia

Synthesis, characterization, and thermal behavior of amidosulfonates of transition metals in air and nitrogen atmosphere

Eclética Química, vol. 45, no. 4, 2020, pp. 32-39
Universidade Estadual Paulista Júlio de Mesquita Filho
Brasil

DOI: https://doi.org/10.26850/1678-4618eqj.v45.4.2020.p32-39

Available in: https://www.redalyc.org/articulo.oa?id=42964416003

Eclética Química Journal

Original article
iq.unesp.br/ecletica

| Vol. 45 | n. 4 | 2020 |

Synthesis, characterization, and thermal behavior of amidosulfonates of transition metals in air and nitrogen atmosphere

Jose Marques Luiz[1+], Ronaldo Spezia Nunes[1]

1. São Paulo State University (Unesp), School of Engineering, Department of Chemistry and Energy, Guaratinguetá, São Paulo, Brazil

[+]Corresponding author: Jose Marques Luiz, Phone: +55 12 31232170, Email address: jose-marques.luiz@unesp.br

ARTICLE INFO

Article history:
Received: January 29, 2020
Accepted: May 11, 2020
Published: October 01, 2020

Keywords:
1. sulfamic acid
2. thermal behavior
3. sulfamates
4. transition metals

ABSTRACT: The amidosulfonates of Mn^{2+}, Co^{2+}, Ni^{2+}, Cu^{2+} and Zn^{2+} were prepared by the direct reaction between the metal carbonate and the amidosulfonic acid with heating and stirring. The compounds were characterized by infrared absorption spectroscopy (IRFT), elemental analysis, thermal analysis (TG and DTA) and X-ray diffraction by the powder method. The absorptions observed in IR spectra are associated with N-H and O-H stretching, as well as symmetrical and asymmetric S-O stretching in the sulfonic group. The compounds present X-ray diffraction pattern with well-defined reflections, showing no evidence of isomorphism. The TG-DTA curves allowed to establish the stoichiometry of compounds as $M(NH_2SO_3)_2.xH_2O$, where M = Mn^{2+}, Co^{2+}, Ni^{2+}, Cu^{2+} and Zn^{2+} and x ranging from 1 to 4. Dehydration leads to the formation of stable anhydrous. In all cases the respective sulfates are formed as an intermediate. After consecutive steps of decomposition, the respective oxides were obtained: Mn_3O_4, CoO, NiO, CuO and ZnO. The TG-DTA curves are characteristic for each sample, with thermal events related to dehydration and ligand decomposition.

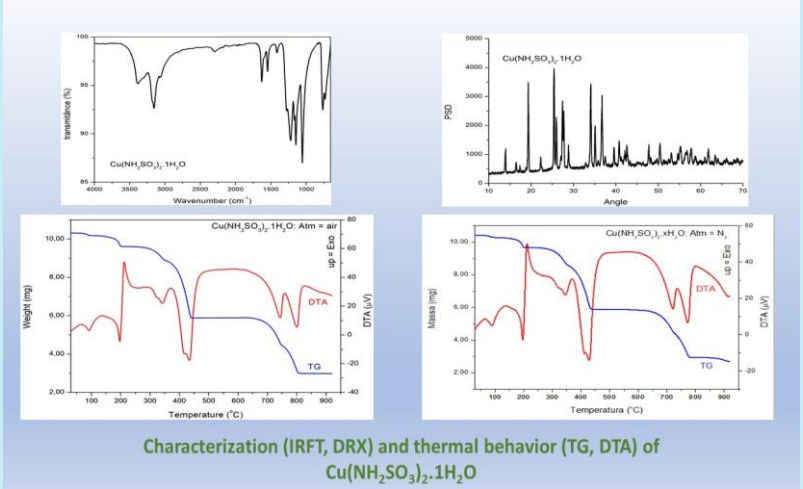

Characterization (IRFT, DRX) and thermal behavior (TG, DTA) of $Cu(NH_2SO_3)_2.1H_2O$

1. Introduction

The amidosulfonic acid or sulfamic acid (NH_2SO_3H) has molar mass 97.10 g mol^{-1}. When dry it is stable, but in solution, it is easily hydrolyzed, forming ammonium bisulfate. It is relatively soluble in water, moderately soluble in alcohol, poorly soluble in acetone, insoluble in ether and very soluble in nitrogenous bases, liquid ammonia, pyridine, formamide and dimethylformamide. It is classified as a strong acid (pH = 1.2 in 1% aqueous solution and 25 ºC). It is used as standard in alkalimetry, in steel cleaning, in removal of nitrites and stabilization of chlorine in pool water. It is a toxic compound, used as poison for rats. Handling requires careful care as it easily irritates the skin and mucous membrane. It forms orthorhombic crystals and has melting point near 205 ºC[1]. In recent years sulfamic acid has been used as an efficient heterogeneous catalyst in a series of organic reactions, such as acetylation, esterification, condensation, transesterification, among others[2]. It is a ZWITTERION, in other words, a dipolar ion having opposite charges on different atoms. In the formation of metal complexes, both amine and sulfonate groups participate in the coordination with the metal ion.

Few studies report the chemical and thermal properties of metal salts containing sulfonic acid derivatives, although the preparation of these salts

is easy to perform[3-10]. Maksin and Standritchuk[3] studied the water solubility of Ni(II) and Co(II) sulfamates. Budurov *et al*.[4,5] studied by DSC the phase transformations that occur in the heating of some amidosulfonates, determining the energy involved in the processes represented by endothermic peaks. Also, by DSC, Thege[6] investigated the thermal behavior of $(NH_4)_2SO_4$, NH_4HSO_4 and $NH_4NH_2SO_3$. The crystalline structure and growth of $Li[NH_2SO_3]$ monocrystals was studied by Stade, Held and Bohaty[7], and it was possible to establish the spatial group, cell parameters and refractive index for the crystals obtained. The elastic properties of sulfamic acid and various sulfamates were studied by Haussül and Haussül and reported phase transformations[8]. Shimizau *et al*.[9] determined the crystallographic properties of silver amidosulfonate and described a lamellar structure with potential chemical applications. Squattrito and coworkers studied the layered structures of metal salts of sulfonic acid derivatives[10-12]. Jaishree *et al*.[13] studied the optical and thermal properties of a monocrystal of amidosulfonic acid and reported the absorption bands in the infrared region. The main absorptions were attributed to the vibrational modes of the $-SO_3^-$ and $-NH_3^+$ group. Brahmaji *et al*. also identified the functional groups by FTIR and reported the changes observed in the pure crystals and doped with Tb^{3+} [14]. Wickleder[15] studied the synthesis, crystal structure, and thermal behavior of some rare earth amidosulfonates. Luiz, Nunes and Matos[16] studied the thermal behavior of all the amidosulfonates of the rare earth series and observed a mass gain between 250 °C and 350 °C, attributed to an oxidative process $SO_3^{2-} \rightarrow SO_4^{2-}$, which is more evident in a lower heating rate. Brahmaji *et al*.[14] also observed mass gain in this temperature range.

2. Materials and Methods

All chemicals used in this study were of analytical grade. Metallic chlorides were obtained from Sigma Aldrich, while the sodium hydrogen carbonate and silver nitrate were obtained from Merck and were used without further purification.

2.1 Metal Carbonates

Carbonates of Mn(II), Co(II), Ni(II), Cu(II) and Zn(II) were prepared by adding slowly, with continuous stirring, a saturated sodium hydrogen carbonate solution to aqueous solutions metal chloride, until total precipitation of the metal ions. The precipitates were washed with distilled water until the elimination of chloride ions (qualitative test with $AgNO_3/HNO_3$ solution for chloride) and was placed in vacuum desiccator until constant mass.

2.2 Metal Amidosulfonates

The compounds were prepared by the direct reaction between the aqueous suspension of the metal carbonates (Mn, Co, Ni, Cu and Zn) and the amidosulfonic acid, with heating at 80 °C and stirring. The acid in powder form was slowly added until a small amount of the metal carbonate remained. The carbonate in excess was removed by filtration and the aqueous solution was evaporated slowly near to dryness. Subsequently, the solution was kept in vacuum desiccator until constant mass.

2.3 Characterization of samples

The infrared spectroscopy for amidosulfonic acid and its metal amidosulfonates were run on a Perkin-Elmer Spectrum 100 ATR FTIR spectrophotometer using ATR accessory with germanium crystal. The FTIR spectra were recorded with 16 scans per spectrum a resolution of 4 cm^{-1}.

The X-ray powder patterns were obtained by using a BRUKER System D8 Advance Diffractometer, employing CuKα radiation (λ = 1.541 Å), 25 mA, 40 kV, 10 rpm rotation, 0.02 step, 0.6 slit mm, time 0.3 s, in the range 2θ from 10 to 70 degrees. Elemental analysis for H, N and S was performed using a Leco CHNS Analyzer.

The thermal behavior was evaluated by thermogravimetry (TG) and differential thermal analysis (DTA) in the simultaneous module TG-DTA 6200 Extar 6000 from Seiko SII, with sample mass of the order of 3 to 10 mg, heating ratio ß = 20 °C min^{-1} (30 to 900 °C), alumina crucible, dynamic atmosphere of synthetic air and nitrogen, with flow of 100 mL min^{-1}. As reference for DTA, previously calcined alumina was used.

Eclética Química Journal, vol. 45, n. 4, 2020, 32-39
ISSN: 1678-4618
DOI: 10.26850/1678-4618eqj.v45.4.2020.p32-39

3. Results and discussion

The elemental analysis results are presented in Tab. 1 and are in agreement with the proposed general formula $M(NH_2SO_3)_2.xH_2O$, where M = Mn^{2+}, Co^{2+}, Ni^{2+}, Cu^{2+} and Zn^{2+} and x the number of water molecules ranging from 1 to 4, where x = 4 for Mn^{2+}, 3 for Co^{2+} and Zn^{2+}, 2 for Ni^{2+} and 1 for Cu^{2+}.

Table 1. Elemental analysis of the solid compounds.

Compound	% N		% H		% S	
	Calc.	EA	Calc.	EA	Calc.	EA
$Mn(NH_2SO_3)_2.4H_2O$	8.78	8.77	3.80	3.79	20.10	20.08
$Co(NH_2SO_3)_2.3H_2O$	9.18	9.31	3.30	3.54	20.01	21.30
$Ni(NH_2SO_3)_2.2H_2O$	9.76	9.63	2.81	2.78	22.36	22.04
$Cu(NH_2SO_3)_2.1H_2O$	10.24	10.20	2.21	2.21	23.43	23.35
$Zn(NH_2SO_3)_2.3H_2O$	8.99	9.08	3.24	3.27	20.58	20.78

The main infrared absorption bands were associated with the N-H stretching, namely, a NH_3^+ broad band at 3400-3300 cm^{-1}, the N-H stretching as a weak band at 2873 cm^{-1} and the absorptions observed at 1533 and 1433 cm^{-1} due to symmetric stretching mode of NH_3^+ while at 1567 cm^{-1} is due to asymmetric mode. The SO_3^- stretching vibration was observed in a 1065 cm^{-1} and at 685 cm^{-1}, the N-S stretching mode can be seen, all these absorptions agree with the literature[4-14]. The absence of that weak band of N-H stretching is an evidence that de coordination of the metal ions occurred by NH_3^+ group. Another fact is the increase observed in the wavenumber for the N-S stretching, suggesting that the N-S bond becomes strongest. The vibrational spectra in the infrared region of amidosulfonic acid and metal amidosulfonates are show in the Fig. 1.

The X-ray powder pattern of the metal amidosulfonates are shown in the Fig. 2. The X-ray diffractograms indicate that the compounds were obtained with a certain crystallinity degree, showing no evidence of isomorphism. The compounds showed low relative intensity (I_o) reflections: Mn (2θ = 19.0; I_o = 845); Co (2θ = 19.3; I_o = 3621); Ni (2θ = 26.3; I_o = 6534); Cu (2θ = 25.4; I_o = 4010); Zn (2θ = 19.4; I_o = 4146).

By the TG/DTA curves it was possible to establish the stoichiometry of the compounds, such as: $ML_2.xH_2O$, where M represents the metallic ions M = Mn^{2+}, Co^{2+}, Ni^{2+}, Cu^{2+} and Zn^{2+}; L represents the anion $NH_2SO_3^-$ and x the number of water molecules ranging from 1 to 4, where x = 4 for Mn^{2+}, 3 for Co^{2+} and Zn^{2+}, 2 for Ni^{2+} and 1 for Cu^{2+}. In a synthetic air atmosphere, the events associated with the thermal decomposition of the ligand occur at slightly lower temperatures than in a nitrogen atmosphere. Tables 2 and 3 show the results extracted from the TG and DTA curves in the atmosphere of synthetic air and nitrogen. Figures 3 and 4 show the TG and DTA curves in the atmosphere of synthetic air and nitrogen, respectively.

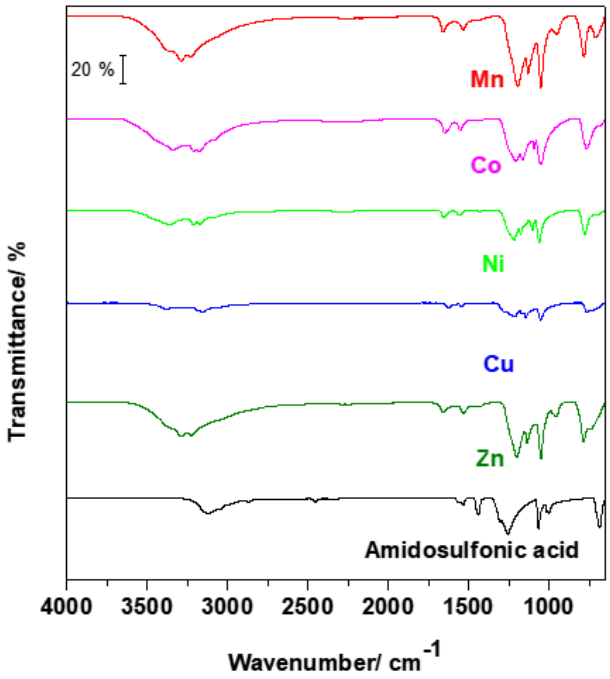

Figure 1. Vibrational spectra in the infrared region of amidosulfonic acid and metal amidosulfonates.

Eclética Química Journal, vol. 45, n. 4, 2020, 32-39
ISSN: 1678-4618
DOI: 10.26850/1678-4618eqj.v45.4.2020.p32-39

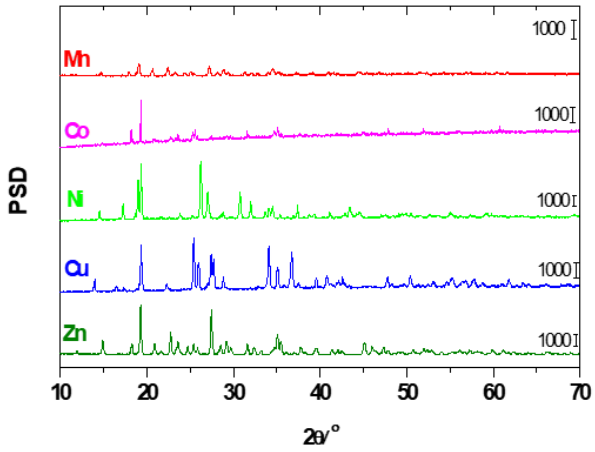

Figure 2. X-ray diffraction pattern of the metal amidosulfonates.

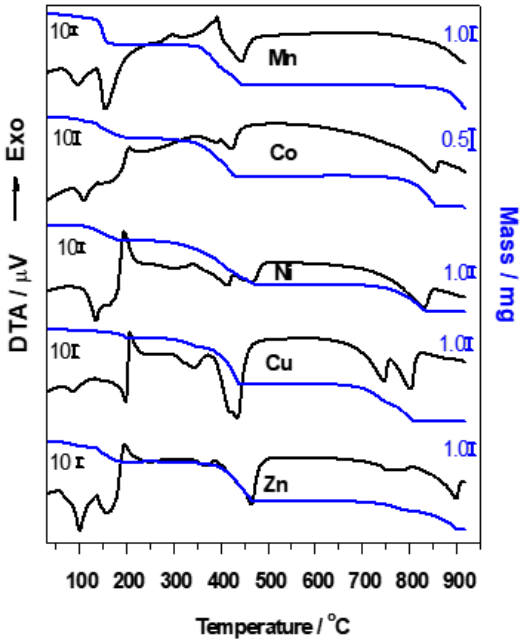

Figure 3. TG and DTA curves of the obtained compounds, in a synthetic air atmosphere. Sample mass: Mn = 9.680 mg, Co = 2.980 mg, Ni = 10.194 mg, Cu = 10.314 mg and Zn = 10.064 mg.

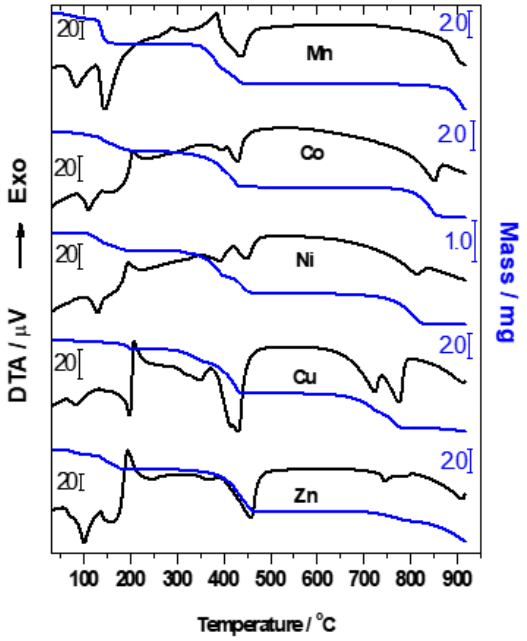

Figure 4. TG and DTA curves of the obtained compounds, in a nitrogen atmosphere. Sample mass: Mn = 10.383 mg, Co = 3,794 mg, Ni = 2,984 mg, Cu = 10.414 mg and Zn = 10.193 mg.

Table 2. Results extracted from the TG curves.

Samples	Molar mass / g mol^{-1}		Metal / %		H_2O / %		Residue / %		
	Calc.	*TG*	*Calc.*	*TG*	*Calc.*	*TG*	*Calc.*	*TG*	*Oxide*
$Mn(L)_2.4H_2O$ (air) $Mn(L)_2.4H_2O$ (N_2)	319.17	318.99 319.90	17.21	17.22 17.17	22.57	22.58 22.75	?	? ?	Mn_3O_4
$Co(L)_2.3H_2O$ (air) $Co(L)_2.3H_2O$ (N_2)	305.14	301.35 300.79	19.31	19.56 19.59	17.71	16.67 16.52	24.56	24.86 24.91	CoO
$Ni(L)_2.2H_2O$ (air) $Ni(L)_2.2H_2O$ (N_2)	286.90	290.40 291.72	20.46	20.21 20.11	12.55	13.61 14.00	26.03	25.77 25.60	NiO
$Cu(L)_2.1H_2O$ (air) $Cu(L)_2.1H_2O$ (N_2)	273.75	274.58 274.81	23.21	23.15 23.13	6.58	6.86 6.94	29.06	28.93 28.95	CuO
$Zn(L)_2.3H_2O$ (air) $Zn(L)_2.3H_2O$ (N_2)	311.61	309.07 308.32	20.98	21.16 21.21	17.34	17.66 16.46	26.12	26.33 ?	ZnO

Eclética Química Journal, vol. 45, n. 4, 2020, 32-39
ISSN: 1678-4618
DOI: 10.26850/1678-4618eqj.v45.4.2020.p32-39

Table 3. Results extracted from the DTA curves.

Samples	DTA Peak (Tp) / ºC								
	endo	***endo***	***exo***	***exo***	***endo***	***endo***	***endo***	***endo***	***endo***
$Mn(L_2).4H_2O$ (air)	89.59	148.4	289.0	387.2	439.4	671.3	874.0		
$Mn(L_2)_2.4H_2O$ (N_2)	84.64	146.8	289.0	383.8	439.4	699.4	872.8		
$Co(L)_2.3H_2O$ (air)	112.4	156.5	210.5		392.0	426.4	854.8		
$Co(L)_2.3H_2O$ (N_2)	110.8	164.8	209.0		400.2	432.9	853.2		
$Ni(L)_2.2H_2O$ (air)	133.9	164.2	203.0		303.4	411.3	462.0	824.1	
$Ni(L)_2.2H_2O$ (N_2)	132.0		200.7		323.6	395.3	450.0	814.0	
$Cu(L)_2.1H_2O$ (air)	89.60	195.9	210.5		343.0	419.8	436.2	741.9	799.1
$Cu(L)_2.1H_2O$ (N_2)	89.60	195.9	212.4		344.6	411.7	426.4	719.2	773.0
$Zn(L)_2.3H_2O$ (air)	97.10	162.1	203.0		364.2	457.4	804.2	900.0	
$Zn(L)_2.3H_2O$ (N_2)	97.10	164.8	201.6		364.2	465.4	789.4	912.0	

3.1 $Mn(NH_2 SO_3)_2.4H_2O$

Dehydration of the manganese (II) amidosulfonate occurs in two consecutive steps with the elimination of one and subsequently three water molecules, between 30 and 220 °C, with mass loss about 22 %. In this step two endothermic peaks are observed at 90 ºC and 148ºC (synthetic air) at 85 ºC and 147 ºC (N_2). The anhydrous compound remains stable between 219 ºC and 340 ºC (synthetic air) and between 197 ºC and 333 ºC (N_2). Although no mass change was observed in this temperature range, there is an exothermic peak at 289 ºC (synthetic air and N_2) which may be associated with a crystallization process. Brahmaji *et al.*[14] also reported a gain mass in this range temperature, however this thermal event needs to be further investigated. Budurov *et al.*[5] reported endothermic peaks attributed to phase transition at 177 ºC (KNH_2SO_3) and 182 ºC ($NaNH_2SO_3$). Haussühl and Haussühl[8] also detected phase transformation in $CsNH_2SO_3$.

The thermal decomposition of the compounds occurs in two distinct steps. The first step begins with an exothermic (386 ºC) process followed by another endotherm (439 ºC) at both atmospheres. This stage leads to the formation of an intermediate, stable over a wide temperature range: 450 ºC to 800 ºC (synthetic air) and 443 ºC and 820 ºC (N_2). This intermediate is probably $MnSO_4$ (Calc. = 47.31 %, TG = 47.34 %), that begins to decompose with an endothermic event (850 ºC) to produce the oxide. In the temperature range in which the experiments were performed (30 ºC → 900 ºC) the formation of the residual oxide could not be observed.

3.2 $Co(NH_2SO_3)_2.3H_2O$

The dehydration process of the cobalt (II) amidosulfonate occurs in a single step, with simultaneous elimination of three water molecules between 85 and 220 ºC and loss of mass of 16.6%. In this stage two endothermic peak are observed around 112 ºC and 157 ºC (synthetic air) and 111 ºC and 164 ºC (N_2). After the anhydrous formation, an exothermic peak is observed around 210 ºC, which may be associated with a crystallization process. The decomposition of the ligand occurs in two distinct stages: between 245ºC and 450 ºC (synthetic air) and between 258 ºC and 442 ºC (N_2), both with formation of the $CoSO_4$ intermediate. In this step two endothermic DTA peaks are observed: 392 ºC and 426 ºC (synthetic air) and 400 ºC and 433 ºC (N_2). The $CoSO_4$ intermediate (Calc. = 50.80 %, TG = 51.80 %) remains stable over a wide temperature range: between 442 ºC and 720 ºC (synthetic air) and between 450 ºC and 716 ºC (N_2). The formation of the residue occurs at 861 ºC, with mass loss of the order of 26 %, compatible with the formation of CoO, in both atmospheres.

3.3 $Ni(NH_2SO_3)_2.2H_2O$

The dehydration of the nickel (II) amidosulfonate occurs in a two overlapping steps, with elimination of two water molecules between 90 and 192 ºC (synthetic air) between 100 ºC and 206 ºC (N_2) with mass loss of order of 13.5 %. At this stage, endothermic peaks are observed at 134 ºC and 164 ºC (synthetic air) and 132 ºC (N_2). After the anhydrous formation, an intense exothermic peak is observed at 203 ºC (synthetic

Eclética Química Journal, vol. 45, n. 4, 2020, 32-39
ISSN: 1678-4618
DOI: 10.26850/1678-4618eqj.v45.4.2020.p32-39

air) and 201 ºC (N_2) of low intensity, which may be associated with a crystallization process. The decomposition of the ligand occurs in two distinct stages: between 251 ºC and 479 ºC (synthetic air) and between 294 ºC and 461 ºC (N_2), both with formation of the $NiSO_4$ intermediate. In this stage endothermic DTA peaks are observed at: 304 ºC, 411 ºC and 462 ºC (synthetic air) and 324 ºC, 395 ºC and 450 ºC (N_2). The $NiSO_4$ intermediate (Calc. = 53.94 %, TG = 53.30 %) remains stable over a wide temperature range: between 474 ºC and 720 ºC (synthetic air) and between 459 ºC and 716 ºC (N_2). The formation of the residue occurs at 831 ºC (synthetic air and N_2) with loss mass in the order of 26 %, compatible with the formation of NiO, in both atmospheres.

3.4 $Cu(NH_2SO_3)_2.1H_2O$

The dehydration of the copper (II) amidosulfonate occurs in a two overlapping steps, eliminating one water molecule between 73 ºC and 199 ºC (synthetic air) and between 65 ºC and 203 ºC (N_2) with mass loss of 6.9 % in both atmospheres. At this stage, two endothermic peaks were observed at 89.6 ºC and 196 ºC in both atmospheres. After the anhydrous formation, an exothermic peak around 211 ºC (synthetic air and N_2) of low intensity is observed, which may be associated with a crystallization process. The decomposition of the ligand occurs in two distinct stages: between 200 ºC and 450 ºC (synthetic air) and between 206 ºC and 440 ºC (N_2), both with formation of the $CuSO_4$ intermediate (Calc. = 58.31 %, TG = 58.13 %). In this stage endothermic DTA peaks are observed: 343 ºC, 420 ºC and 436 ºC (synthetic air) and 345 ºC, 412 ºC and 426 ºC (N_2). The $CuSO_4$ intermediate remains stable over a wide temperature range: between 444 ºC and 694 ºC (synthetic air) and between 440 ºC and 618 ºC (N_2). In this stage endothermic peaks are observed at 741 ºC and 799 ºC (synthetic air) and 718 ºC and 773 ºC (N_2). The formation of the residue supposed CuO occurs at 810 ºC (synthetic air) and 780 ºC (N_2). Under N_2 atmosphere a new stage of mass loss appears, which begins at 840 ºC and probably ends at temperatures above 900 ºC. The DTA profile of the beginning of this stage has endothermic characteristics, suggesting a $Cu^{2+} \rightarrow Cu^{+}$ reduction process.

3.5 $Zn(NH_2SO_3)_2.3H_2O$

Dehydration $Zn(NH_2SO_3)_2.3H_2O$ occurs two overlapping steps, between 64 °C and 195 °C (synthetic air and N_2), equivalent to the consecutive release of one and two water molecules, respectively, with losses of the order of 17 %, Endothermic peaks are observed at 97 ºC and 163 ºC (synthetic air and N_2). After formation of the anhydrous compounds, an exothermic peak was observed around 202 ºC (synthetic air and N_2). The anhydrous compound remains stable between 190 °C and 295 °C (synthetic air) and 196 °C and 322 °C (N_2). The decomposition of the ligand in synthetic air starts at 304 ºC, with endothermic peaks at 364 ºC and 457 ºC (synthetic air) and 364 ºC and 465 ºC (N_2). This stage leads to the formation of intermediate $ZnSO_4$ (Calc. = 51.80 %, TG = 52.40 %), which remains stable over a wide temperature range of 467 ºC to 688 ºC (synthetic air) and 471 ºC to 684 ºC (N_2). In a synthetic air atmosphere, the decomposition to ZnO occurs from 690 ºC and ends at 913 ºC, presenting endothermic peaks at 804 ºC and 900 ºC. In nitrogen atmosphere, residual oxide formation is not completed until 920 ºC and endothermic peaks are observed at 744 ºC, 789 ºC and 912 ºC.

4. Conclusions

The main absorptions in the infrared: *νO-H* (3600 - 2700 cm^{-1}) in the salts; *νN-H* (3400-3300 cm^{-1}) in amidosulfonic acid; *νsS-O* (1260-1140 cm^{-1}) and *νasS-O* (1040-1020 cm^{-1}) emphasize the differences between the spectra of the salts and of the amidosulfonic acid, evidence the bond to the metal suggesting that the coordination occurs by the sulphonic grouping.

The X-ray diffractograms indicate that the compounds were obtained with a certain crystallinity degree, showing no evidence of isomorphism. The compounds showed relatively low intensity reflections.

The thermoanalytical results (TG/DTA) allowed to establish the stoichiometry of the compounds as: $ML_2.xH_2O$, where M represents the metallic ions Mn^{2+}, Co^{2+}, Ni^{2+}, Cu^{2+} and Zn^{2+}; L represents the anion $NH_2SO_3^-$; x represents the number of water molecules, where x = 4 for Mn^{2+}, x = 3 for Co^{2+}; and Zn^{2+}, x = 2 for Ni^{2+} and x = 1 for Cu^{2+}. No significant differences were observed

Eclética Química Journal, vol. 45, n. 4, 2020, 32-39
ISSN: 1678-4618
DOI: 10.26850/1678-4618eqj.v45.4.2020.p32-39

between the analysis carried out in synthetic air or nitrogen atmosphere, only the thermal decomposition of the ligand in synthetic air atmosphere occur at slightly lower temperatures that in a nitrogen atmosphere. For all compounds, the MSO_4 stable intermediate was observed, which later decomposes to the respective oxide, that is: Mn_3O_4, CoO, NiO, CuO and ZnO. In some samples the residual oxide is produced at temperatures above 950 ºC.

Acknowledgments

This research was supported by resources supplied by the Faculdade de Engenharia de Guaratinguetá (UNESP). The authors thank Prof. Dr. Edson Cocchieri Botelho (DMT-FEG-UNESP) for TG–DTA measurements, Prof. Dr. Sergio Francisco dos Santos (DMT-FEG-UNESP) for X-ray diffractometry, Prof. Dr. Konstantin Georgiev Kostov (DFI-FEG-UNESP) for FTIR measurements.

References

[1] Index, M., Centennial edition, Merck & Co. Inc. Rahway, 1989.

[2] Kamal, A., Babu, K. S., Hussaini, S. M. A., Srikanth, P. S., Balakrishna, M., Alarifi, A., Sulfamic acid: an efficient and recyclable solid acid catalyst for the synthesis of 4,5-dihydropyrrolo[1,2-*a*]quinoxalines, Tetrahedron Letters 56 (31) (2015) 4619-4622. https://doi.org/10.1016/j.tetlet.2015.06.006.

[3] Maksin, V. I., Standritchuk, O. Z., Solubility diagrams of the systems nickel sulfamate-water and cobalt sulfamate-water, Russian Journal of Applied Chemistry 80 (7) (2007) 1048-1054. https://doi.org/10.1134/S1070427207070063.

[4] Budurov, S, Tzolova, G., Thermogravimetrische Untersuchung der thermischen Zersetzung von Amidosulfonaten einwertiger metalle, Thermochimica Acta 303 (1) (1997) 101-105. https://doi.org/10.1016/S0040-6031(97)00256-6.

[5] Budurov, S., Tzolova, G., Bohatý, L., New structural phase transitions in potassium and sodium amidosulfonates, Thermochimica Acta 307 (1) (1997) 91-96. https://doi.org/10.1016/S0040-6031(97)00360-2.

[6] Thege, I. K., DSC investigation of the thermal behaviour of $(NH_4)_2SO_4$, NH_4HSO_4 and $NH_4NH_2SO_3$, Thermochimica Acta 60 (2) (1983) 149-159. https://doi.org/10.1016/0040-6031(83)80265-2.

[7] Stade, J., Held, P., Bohatý, L., Crystal Growth, Crystal Structure and Physical Properties of Lithium Sulfamate $Li[NH_2SO_3]$, Crystal Research and Technology 36 (4-5) (2001) 347-360. https://doi.org/10.1002/1521-4079(200106)36:4/5%3C347::AID-CRAT347%3E3.0.CO;2-Q.

[8] Haussühl, E., Haussühl, S., Elastic properties of sulfamic acid and sulfamates of Li, Na, K, Rb, Cs, Tl, NH_4, $C(NH_2)_3$ and $(CH_3)_3NCH_2COOH$, Zeitschrift Für Kristallografie 210 (4) (1995) 269-275. https://doi.org/10.1524/zkri.1995.210.4.269.

[9] Shimizau, G. K. H., Enright, G. D., Ratclife, C. I., Rego, G. S., Reid, J. L., Ripmeester, J. A., Silver Sulfonates: An Unexplored Class of Layered Solids, Chemistry of Materials 10 (11) (1998) 3282-3283. https://doi.org/10.1021/cm980409b.

[10] Shubnell, A. J., Kosnic, E. J., Squattrito, P. J., Structures of layered metal sulfonate salts: trends in coordination behavior of alkali, alkaline earth and transition metals, Inorganica Chimica Acta 216 (1-2) (1994) 102-112. https://doi.org/10.1016/0020-1693(93)03700-K.

[11] Gunderman, B. J., Squatrito, P. J., Synthesis and Structures of Potassium and Rubidium Arenesulfonates, Journal Logo 33 (13) (1994) 2924-2931. https://doi.org/10.1021/ic00091a035.

[12] Kosnic, E. J., McClymont, E. L., Hodder, R. A., Squattrito, P. J., Synthesis and structures of layered metal sulfonate salts, Inorganica Chimica Acta 201 (2) (1992) 143-151. https://doi.org/10.1016/S0020-1693(00)85325-6.

[13] Jaishree, D., Kanchana, G., Kesavasamy, R., Investigations on Growth, Optical and Thermal Properties of Sulphamic Acid Single Crystals, Investigations on Growth, Optical and Thermal Properties of Sulphamic Acid Single Crystals 2014 (2014) 950467. https://doi.org/10.1155/2014/950467.

[14] Brahmaji, B., Rajyalakshmi, S., Rao, T. K. V., Valluru S. R., Basha, S. K. E., Satyakamal, C., Veeraiah, V., Rao, K. R., Tb^{3+} added sulfamic acid single crystals with optimal photoluminescence properties for opto-electric devices, Journal of Science: Advanced Materials and Devices 3 (1) (2018) 68-76. https://doi.org/10.1016/j.jsamd.2017.12.002.

[15] Wickleder, M. S., Syntheses, crystal structures, and thermal behavior of the rare earth amidosulfates

$M(NH_2SO_3)_3 \cdot 2H_2O$ (M=Pr, Nd, Sm), Journal of Alloys and Compounds 303-304 (2000) 445-453. https://doi.org/10.1016/S0925-8388(00)00624-1.

[16] Luiz, J. M., Nunes, R. S., Matos, J. R., Síntese, caracterização e comportamento térmico de amidossulfonatos de terras raras, Quimica Nova 36 (3) (2013) 426-430. https://doi.org/10.1590/S0100-40422013000300013.

Eclética Química Journal, vol. 45, n. 4, 2020, 32-39
ISSN: 1678-4618
DOI: 10.26850/1678-4618eqj.v45.4.2020.p32-39